

van der Waals Interaction Energies between Non-Planar Bodies

Eun-Suok Oh[†]

Department of Aerospace Engineering, Texas A&M University, College Station, TX 77843-3141, USA
(Received 14 October 2003 • accepted 20 December 2003)

Abstract—The van der Waals interaction energies between non-planar geometries are obtained without the assumption that the distance between two non-planar bodies is much smaller than radii of the non-planar bodies. Based on atom-to-body van der Waals energies, we calculate body-to-body van der Waals interaction energies for several non-planar geometries. Using the continuum approach, we discuss the van der Waals interactions in two-dimensional carbon nanotubes and C₆₀ molecules.

Key words: van der Waals Interaction, Non-Planar Body, Carbon Nanotube, C₆₀, Peapods

INTRODUCTION

For two non-polar molecules separated by a distance 2 Å. 100 Å, there always exists a long-range interaction, which is generally known as the van der Waals interaction or the London dispersion interaction. Forces due to the van der Waals interaction play an important role in various phenomena such as adhesion, adsorption, surface tension, transport in porous media, wetting, etc. [Israelachvili, 1973; Hough and White, 1980; Adamczyk and van de Ven, 1981; Chang and Wang, 1996; Bhattacharjee and Sharma, 1996, 1997; Gu and Li, 2002]. Recently, the van der Waals interaction in nanoscale materials such as carbon nanotubes and nanowires has been studied due to the wide variety of potential applications of nanoscale materials [Henrard et al., 1999; Qian et al., 2001; Mendeleev et al., 2002; Boustimi et al., 2002, 2003; Ulbricht et al., 2003].

Carbon nanotubes (CNTs), discovered by Iijima [1991], possess remarkable electrical, mechanical, and thermal properties [Yakobson et al., 1996; Wildoer et al., 1998; Odom et al., 1998; Yu et al., 2000]. For example, CNTs are 100 times stronger and 6 times lighter than steel. They are composed of two-dimensional hexagonal ring structures formed by rolling up graphene sheets. Morphologically, a single-walled carbon nanotube (SWCNT) can be idealized as a single rolled-up sheet of graphite, and a multi-walled carbon nanotube (MWCNT) as one containing many such co-axial tubes of varying diameter. At normal conditions, CNTs exist in bundle form (or rope) in which each CNT is tied by the van der Waals interaction, and are randomly oriented as shown in Fig. 1.

The van der Waals interaction is also a key issue in understanding the mechanics of C₆₀ (buckminster fullerene) and that of flow of water molecules through CNTs [Qian et al., 2001; Hummer et al., 2001]. It is very important in nanoscale CNT mechanics to exactly estimate the van der Waals interactions between non-planar bodies like cylindrical CNTs and spherical C₆₀ molecules.

In calculating the van der Waals interaction energies between non-planar bodies, the following assumption has been normally used:

[†]To whom correspondence should be addressed.

E-mail: esoh@tamu.edu

[‡]This paper is dedicated to Professor Hyun-Ku Rhee on the occasion of his retirement from Seoul National University.

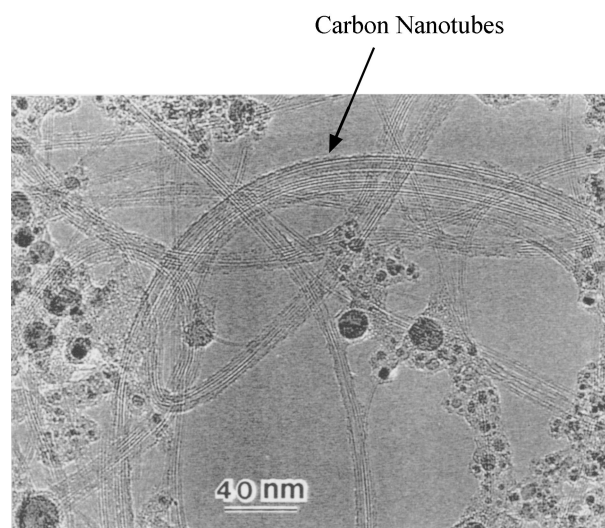


Fig. 1. A high-resolution electron micrograph showing raft-like bundles of single-walled carbon nanotubes [Qin and Iijima, 1997].

the distance between two non-planar bodies is much smaller than radii of the non-planar bodies [Israelachvili, 1991]. This assumption is no longer valid at the nanoscale. Gu and Li [1999] calculated the van der Waals interaction between a spherical particle and a cylinder in terms of the ratio of the separation distance to the radius of the sphere. However, they assumed that all of the molecules on a thin circular disk of the sphere, parallel to the cylinder, are at the same distance away from the cylinder surface.

In this paper, the van der Waals interaction energies between non-planar geometries are obtained without using the above assumptions. We first calculate the atom-to-cylindrical body interaction energies using the attractive term of the Lennard-Jones potential. The body-to-body interaction energies for several non-planar geometries are then obtained by using the atom-to-body interaction energies. In a similar way, we discuss the van der Waals interaction energies for two-dimensional cylindrical carbon nanotubes and spherical C₆₀ molecules.

THEORY

If we consider an atom or a molecule at position \mathbf{r}_i and an atom or a molecule at position \mathbf{r}_j that are sufficiently close together, there exists a long-range intermolecular interaction acting between these two atoms. The Lennard-Jones potential is commonly recommended for non-polar molecules such as methane [Hirschfelder et al., 1954]:

$$\phi(r_{ij}) = 4\epsilon \left[\left(\frac{\sigma}{r_{ij}} \right)^{12} - \left(\frac{\sigma}{r_{ij}} \right)^6 \right] \quad (1)$$

where r_{ij} is the distance between the two atoms or the two molecules. The parameters ϵ and σ represent the collision diameter and well depth, respectively, which can be determined by using the second virial coefficient and viscosity measurements [Hirschfelder et al., 1954]. The r^{-6} term describes attractive forces known as dispersion forces (London forces or induced dipole-induced dipole forces) [Israelachvili, 1991]. The r^{-12} contribution represents short-range repulsive forces.

The non-retarded van der Waals energy between two atoms or two molecules separated by a distance r has been generally estimated by using the attractive term of the Lennard-Jones potential:

$$\phi(r) = -\frac{C}{r^6} \quad (2)$$

where C is the London dispersion force coefficient. Note that with increasing r , the attractive force decays even faster than r^{-6} , approaching r^{-7} . This is referred to as the retardation effect [Israelachvili, 1991].

In estimating the interaction energy between an atom and a macroscopic body or between two macroscopic bodies, we will assume that the intermolecular potential is pairwise additive. This means that the total energy of an atom and a body is the sum of its pair potentials with all of the molecules in the body--an assumption that has been used by several authors [Hamaker, 1937; Mahanty and Ninham, 1976; Israelachvili, 1991]. For condensed media this is not correct, because it ignores the influence of neighboring material on the interaction potentials between the materials at any pair of points.

In order to avoid the assumption of pairwise additivity, Lifshitz [1956] developed what we now refer to as Lifshitz theory by describing the interaction between bodies in the fluctuating electromagnetic field created by the material. Dzyaloshinskii et al. [1961] generalized the Lifshitz theory, using the quantum field theory. Based on the Lifshitz theory, one can calculate the Hamaker constants [Hamaker, 1937] used in expressing the van der Waals interaction energy between two bodies, or an atom and a body. More details are described in the book of Israelachvili [1991].

ATOM-TO-BODY INTERACTION ENERGY

1. Interaction between an Atom and a Cylinder

As shown in Fig. 2(a), an atom at a distance d away from the surface of a cylinder of radius R interacts with the cylinder. The number of molecules in an infinitesimal differential element located on a surface $z=\text{constant}$ is $\rho dx dy dz$, where ρ is the constant number density of molecules in the cylinder.

Since the distance between the atom and the differential element is $\sqrt{x^2 + y^2 + (z+d)^2}$, the interaction energy between the atom and the differential element is, using (2),

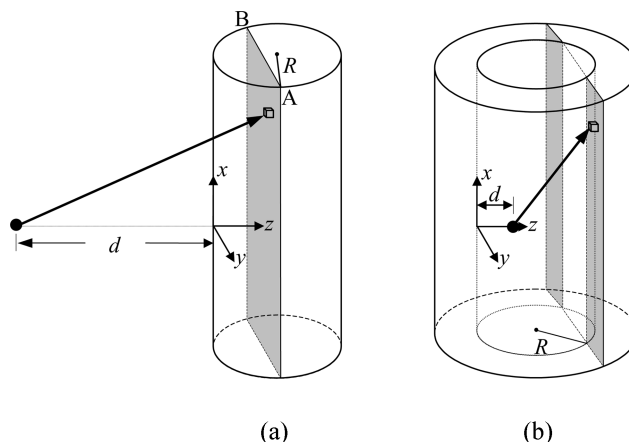


Fig. 2. van der Waals interactions (a) between an atom and a cylinder, and (b) between an atom inside a hollow cylinder and the hollow cylinder. The shadowed areas indicate planes on which $z=\text{constant}$.

$$d\phi_c = -\frac{\rho C}{[x^2 + y^2 + (z+d)^2]^3} dx dy dz \quad (3)$$

In view of the pairwise additivity, the total interaction energy between the atom and the cylinder can be estimated by the volume integration of (3) over the cylinder. The length of \overline{AB} is $2\sqrt{(2R-z)z}$. If the cylinder is assumed to be infinitely long, the total interaction energy is

$$\begin{aligned} \phi_c(d, R) &= \int_0^{2R} \int_{-\sqrt{(2R-z)z}}^{\sqrt{(2R-z)z}} \int_{-\infty}^{\infty} -\frac{\rho C}{\{x^2 + y^2 + (z+d)^2\}^3} dx dy dz \\ &= -\frac{\pi \rho C}{12d^2(d+2R)^3} \left\{ (d^2 + 2dR + 8R^2) \text{Im} \left[E \left[\frac{(d+2R)^2}{d^2} \right] \right] \right. \\ &\quad \left. - 2R(d-2R) K \left[1 - \frac{(d+2R)^2}{d^2} \right] \right\} \quad (4) \end{aligned}$$

Here we have introduced the elliptic integrals of the first kind and the second kind defined as [Abramowitz and Stegun, 1972]

$$\begin{aligned} K[m] &\equiv \int_0^{\pi/2} (1 - m \sin^2 \theta)^{-1/2} d\theta \\ E[m] &\equiv \int_0^{\pi/2} (1 - m \sin^2 \theta)^{1/2} d\theta \quad (5) \end{aligned}$$

In the limit of $d/R \rightarrow 0$, we have

$$\begin{aligned} \lim_{\frac{d}{R} \rightarrow 0} K \left[1 - \frac{(d+2R)^2}{d^2} \right] &= 0 \\ \lim_{\frac{d}{R} \rightarrow 0} E \left[\frac{(d+2R)^2}{d^2} \right] &= \frac{2R}{d} \quad (6) \end{aligned}$$

Thus, Eq. (4) reduces to

$$\phi_c(d) = -\frac{\pi \rho C}{6d^3} \quad (7)$$

which is identical to the net energy between an atom and a planar surface [Israelachvili, 1991]. At a very close distance, the curvature effect on the interaction is negligible.

Using (4), we can calculate the interaction energy of an atom and

a hollow cylinder, whose inner and outer radii are R_i and R_o , respectively. The interaction energy is expressed as

$$\phi(d) = \phi_c(d, R_o) - \phi_c(d, R_i) \tag{8}$$

2. Interaction of an Atom inside a Hollow Cylinder

Now we consider the interaction energy of an atom inside a hollow cylinder whose inner radius is R . A schematic diagram is given in Fig. 2(b). Since the distance between the atom and the differential element in the hollow cylinder is $\sqrt{x^2 + y^2 + (z - d)^2}$, the interaction energy of the atom and the element is

$$d\phi_h = -\frac{\rho C}{[x^2 + y^2 + (z - d)^2]^3} dx dy dz \tag{9}$$

With the pairwise additivity assumption, the total interaction energy of the atom and the hollow cylinder can be written as

$$\begin{aligned} \phi_h(d, R) &= \int_{-\infty}^0 \int_{-\infty}^{\infty} \int_{-\infty}^{\infty} d\phi_h + 2 \int_0^{2R} \int_{-\infty}^{\infty} \int_{-\infty}^{\infty} \frac{d\phi_h}{\sqrt{(2R-z)^2}} + \int_{2R}^{\infty} \int_{-\infty}^{\infty} \int_{-\infty}^{\infty} d\phi_h \\ &= -\frac{\pi \rho C}{6d^3(2R-d)^3} \left\{ \sqrt{(R-d)R} (d^2 - 2dR + 8R^2) \right. \\ &\quad \left. \operatorname{Re} \left(E \left[\frac{(2R-d)^2}{4R(R-d)} \right] \right) + dR(d+2R) K \left[\frac{4(d-R)R}{d^2} \right] \right\} \end{aligned} \tag{10}$$

where the hollow cylinder is assumed to be infinitely long and wide. If the atom is located at the center of the cylinder, *i.e.*, $d=R$, then (10) reduces to

$$\phi_h(d) = -\frac{\pi^2 \rho C}{4d^3} \tag{11}$$

In the limit $d/R \rightarrow 0$, Eq. (10) reduces to (7), which is the interaction energy between an atom and a planer surface.

If the inner and outer radii of the hollow cylinder are R_i and R_o , the net interaction energy can be written as

$$\phi(d) = \phi_h(d, R_o) - \phi_h(d, R_i) \tag{12}$$

BODY-TO-BODY INTERACTION ENERGY

Based on the atom-to-body interaction energies, we will calculate the body-to-body interaction energies for several non-planar geometries. In what follows, we will use the Hamaker constant A defined as

$$A \equiv \pi^2 \rho_1 \rho_2 C \tag{13}$$

where ρ_1 and ρ_2 are the number densities of molecules in bodies 1 and 2, respectively.

1. Interaction between a Hollow Cylinder and an Embedded Solid Cylinder

We first consider the interaction of a hollow cylinder interacting with an embedded solid cylinder as depicted in Fig. 3.

The distance between the differential element in the hollow cylinder and the surface of the embedded cylinder is $r - R_1$. In view of (4), the interaction energy between the element and the embedded cylinder can be expressed as

$$d\Phi_{hc} = \phi_c(r - R_1, R_1) \rho_2 2\pi r dr dz \tag{14}$$

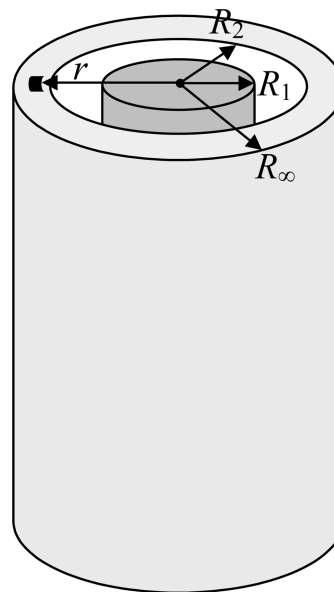


Fig. 3. van der Waals interaction of a hollow cylinder and an embedded solid cylinder.

Thus, the total interaction energy per unit length becomes

$$\begin{aligned} \Phi_{hc} &= \int_{R_2}^{R_1} d\Phi_{hc} \\ &= \int_{R_2}^{R_1} -\frac{A r}{6(r - R_1)^2 (r + R_1)^3} \left\{ [(r - R_1)^2 + 2(r - R_1)R_1 + 8R_1^2] \right. \\ &\quad \left. \operatorname{Im} \left(E \left[\frac{(r + R_1)^2}{(r - R_1)^2} \right] \right) - 2R_1(r - 3R_1) K \left[1 - \frac{(r + R_1)^2}{(r - R_1)^2} \right] \right\} dr \\ &= f \left(\frac{R_o + R_1}{R_o - R_1}, R_1 \right) - f \left(\frac{R_2 + R_1}{R_2 - R_1}, R_1 \right) \end{aligned} \tag{15}$$

in which

$$\begin{aligned} f(k, R_1) &= \frac{A}{192 \pi R_1 k^2} \left\{ 4G_{3,3}^{3,2} (k_{1,1,1}^{2|1.5,1.5,2}) - 4G_{3,3}^{3,2} (k_{10,0,1}^{2|0.5,0.5,2}) \right. \\ &\quad - 2k G_{2,2}^{2,2} (k_{0,0}^{2|0.5,1.5}) + 2k^3 G_{3,3}^{2,3} (k_{0,0,-0.5}^{2|0.5,0.5,0.5}) \\ &\quad + \operatorname{Im} [4\pi^2 k_2 F_1(-0.5, -0.5; 1; k^2)] \\ &\quad + 8\pi^2 k_3^3 F_2(-0.5, 0.5, 0.5; 1, 1.5; k^2) \\ &\quad \left. - \pi k^2 G_{3,3}^{2,2} (-k_{0,0,0}^{2|0.5,1.5,1}) + 2\pi G_{3,3}^{2,2} (-k_{0,1,0}^{2|0.5,1.5,1}) \right\} \end{aligned} \tag{16}$$

Here we have introduced two special functions; a generalized hypergeometric series defined as [Gradshteyn and Ryzhik, 1965]

$${}_p F_q (\alpha_1, \alpha_2, \dots, \alpha_p; \beta_1, \beta_2, \dots, \beta_q; z) \equiv \sum_{n=0}^{\infty} \frac{(\alpha_1)_n (\alpha_2)_n \dots (\alpha_p)_n z^n}{(\beta_1)_n (\beta_2)_n \dots (\beta_q)_n n!} \tag{17}$$

where $(\tau)_n$ is the Pochhammer symbol [Abramowitz and Stegun, 1972]:

$$(\tau)_n \equiv \alpha(\tau+1)(\tau+2)\dots(\tau+n-1) = \frac{\Gamma(\tau+n)}{\Gamma(\tau)} \tag{18}$$

and Meijer's G function defined as [Gradshteyn and Ryzhik, 1965]

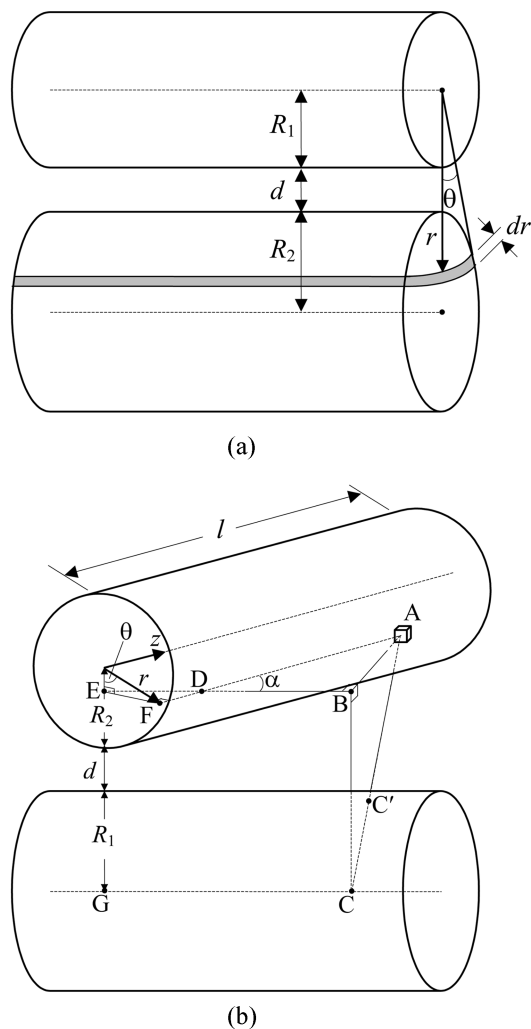


Fig. 4. van der Waals interactions (a) between two parallel cylinders, and (b) between two cylinders crossed at an angle α

$$G_{p,q}^{m,n} \left(\begin{matrix} \alpha_1, \dots, \alpha_p \\ \beta_1, \dots, \beta_q \end{matrix} \right) \equiv \frac{1}{2\pi i} \int \frac{\prod_{j=1}^m \Gamma(\beta_j - s) \prod_{j=1}^n \Gamma(1 - \alpha_j + s)}{\prod_{j=n+1}^p \Gamma(\alpha_j - s) \prod_{j=m+1}^q \Gamma(1 - \beta_j + s)} z^s ds \quad (19)$$

2. Interaction between Two Cylinders

For two parallel cylinders separated by a distance d as shown in Fig. 4(a), we can calculate the interaction energy using (4). Any point in the shadowed area of the illustration is separated by a distance $r - R_1$ from the surface of the cylinder of radius R_1 . Since the number of molecules per unit length in the shadowed area is $\rho_2 2\theta dr$, the interaction energy between two parallel cylinders with a separation distance d becomes

$$\begin{aligned} \Phi_{pc}(d) &= \int_{R_1+d}^{R_1+d+2R_2} \phi_c(r - R_1, R_1) (\rho_2 2\theta r) dr = \int_{R_1+d}^{R_1+d+2R_2} \\ &= \frac{A\theta r}{6\pi(r - R_1)^2 (r + R_1)^3} \left\{ [(r - R_1)^2 + 2(r - R_1)R_1 + 8R_1^2] \right. \\ &\quad \left. \text{Im} \left(E \left[\frac{(r + R_1)^2}{(r - R_1)^2} \right] \right) - 2R_1(r - 3R_1) K \left[1 - \frac{(r + R_1)^2}{(r - R_1)^2} \right] \right\} dr \quad (20) \end{aligned}$$

where

$$\theta \equiv \arccos \left[\frac{r^2 + (R_1 + d + R_2)^2 - R_2^2}{2r(R_1 + d + R_2)} \right] \quad (21)$$

We now calculate the van der Waals energy for a more general case when two cylinders are crossed at an angle α . The illustration is shown in Fig. 4(b). The crossed cylinders are separated by a distance d . First, we need to calculate $\overline{AC'}$, the distance between the differential element in the cylinder of radius R_2 and the surface of the cylinder of radius R_1 . Since \overline{BC} is equal to \overline{EG} , \overline{BC} is $R_1 + d + R_2 - r \cos \theta$. Since \overline{DF} is $r \sin \theta \tan \alpha$, \overline{AB} is $(z - r \sin \theta \tan \alpha) \sin \alpha = z \sin \alpha - r \sin \theta \cos \alpha$. Thus,

$$\overline{AC'} = \sqrt{(R_2 - r \cos \theta + d + R_1)^2 + (z \sin \alpha - r \sin \theta \cos \alpha)^2} - R_1 \quad (22)$$

From (4), the interaction energy between two crossed cylinders can be expressed as

$$\begin{aligned} \Phi_{cc}(d) &= \int_{-l}^l \int_0^{2\pi} \int_0^{R_2} \phi_c(\overline{AC'}, R_1) \rho_2 r dr d\theta dz \\ &= \int_{-l}^l \int_0^{2\pi} \int_0^{R_2} - \frac{Ar}{12\pi(\overline{AC'})^2 (\overline{AC'} + 2R_1)^3} \left\{ [(\overline{AC'})^2 \right. \\ &\quad \left. + 2(\overline{AC'})R_1 + 8R_1^2] \text{Im} \left(E \left[\frac{(\overline{AC'} + 2R_1)^2}{(\overline{AC'})^2} \right] \right) \right. \\ &\quad \left. - 2R_1(\overline{AC'} - 2R_1) K \left[1 - \frac{(\overline{AC'} + 2R_1)^2}{(\overline{AC'})^2} \right] \right\} dr d\theta dz \quad (23) \end{aligned}$$

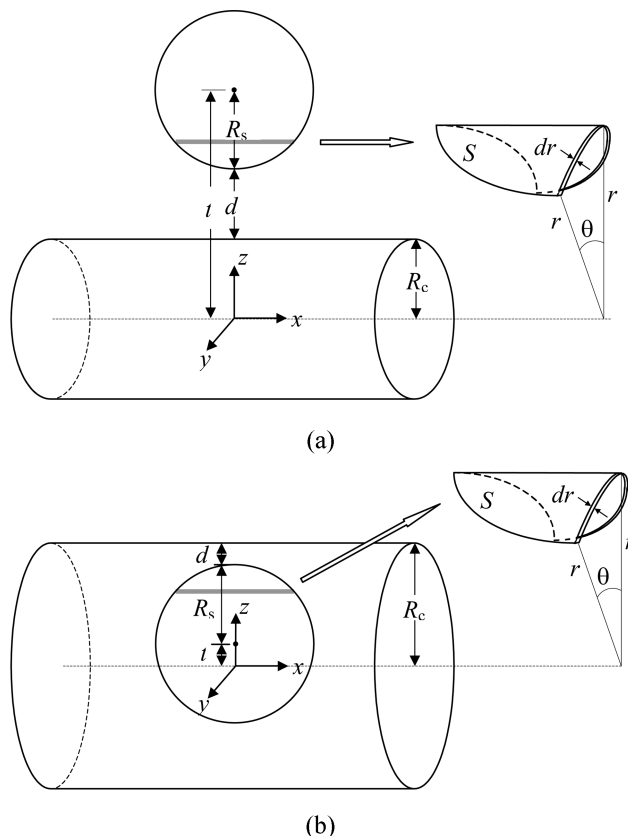


Fig. 5. van der Waals interactions (a) between a cylinder and a sphere, and (b) between a cylinder and a sphere inside the cylinder. The shadowed areas indicate the intersections of a cylinder of radius r and the sphere.

where the length of the cylinder of radius R_c is assumed to be $2l$.

Based on the assumption that the distance between two cylinders is much smaller than the radii of the cylinders, Israelachvili [1991] has given theoretical expressions on the interaction energies for two parallel and crossed cylinders. In fact, the interaction energies calculated by (20) and (23) are equal to those calculated by his results, when $d \ll R_1$ and $d \ll R_2$.

3. Interaction between a Sphere and a Cylinder

In order to calculate the interaction between a cylinder and a sphere as shown in Fig. 5(a), we first determine the intersection S of a cylinder of radius r and a sphere of radius R_s . All of the points on S are at the same distance $r - R_c$ from the surface of the cylinder of radius R_c . S can be determined by solving the following equations simultaneously:

$$y^2 + z^2 = r^2 \tag{24}$$

$$x^2 + y^2 + (z - t)^2 = R_s^2 \tag{25}$$

where t is the center-to-center distance, i.e.,

$$t = R_s + d + R_c \tag{26}$$

The corresponding solutions for x and y are

$$x = \pm \sqrt{R_s^2 - r^2 + 2zt - t^2} \tag{27}$$

$$y = \pm \sqrt{r^2 - z^2} \tag{28}$$

and the intersection is given as [Kaplan, 1991]

$$S = 4 \int x(z) dl = 4 \int_{\cos\theta}^r \sqrt{R_s^2 - r^2 + 2zt - t^2} \sqrt{1 + \left(\frac{dy}{dz}\right)^2} dz$$

$$= 8r \sqrt{(r+t)^2 - R_s^2} \left\{ E \left[\frac{(r-t)^2 - R_s^2}{(r+t)^2 - R_s^2} \right] - K \left[\frac{(r-t)^2 - R_s^2}{(r+t)^2 - R_s^2} \right] \right\} \tag{29}$$

where dl is the arc length element around the surface of the cylinder.

Since all of the molecules in the element volume Sdr are at a distance $r - R_c$ from the surface of the cylinder, using (4), we can express the interaction energy of the sphere and the cylinder as

$$\Phi_{sc}(d) = \int_{r-R_c}^{r+R_s} \int_{r-R_c}^{r+R_s} \phi_c(r - R_c, R_c) \rho_s S dr = \int_{r-R_c}^{r+R_s} \left[\int_{r-R_c}^{r+R_s} 1 - \frac{2Ar\sqrt{(r+t)^2 - R_s^2}}{3\pi(r - R_c)^2(r + R_c)^3} \left\{ E \left[\frac{(r-t)^2 - R_s^2}{(r+t)^2 - R_s^2} \right] - K \left[\frac{(r-t)^2 - R_s^2}{(r+t)^2 - R_s^2} \right] \right\} \times \left\{ (r^2 + 7R_c^2) \text{Im} \left(E \left[\frac{(r - R_c)^2}{(r + R_c)^2} \right] \right) - 2(r - 3R_c) R_c K \left[-\frac{4R_c}{(r + R_c)^2} \right] \right\} dr \right] dr \tag{30}$$

The interaction energies calculated by using (30) for three different radii of the cylinder are compared with previous results given by Gu and Li [1999]. This is shown in Fig. 6. It should be noted that they assumed that all of the molecules on a thin circular disk of the sphere, parallel to the cylinder, are at the same distance away from the cylinder surface. At a relatively big cylinder $R_c/R_s=100$, the interaction energies obtained by both our and Gu and Li's analyses are equal to the energy between the sphere and a flat surface

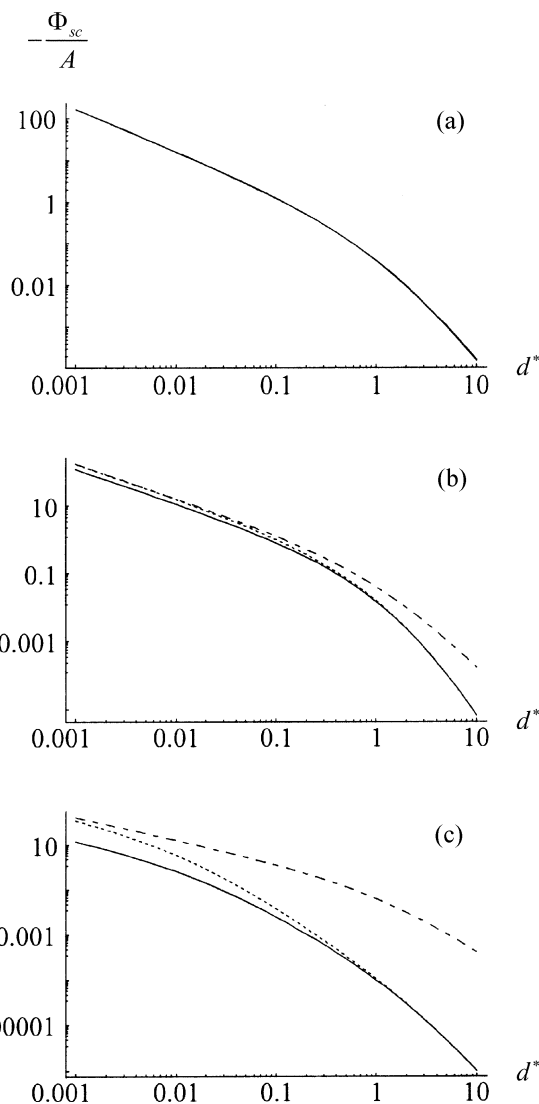


Fig. 6. van der Waals interaction energy of a sphere of radius R_s and a cylinder of radius R_c : (a) $R_c/R_s=100$, (b) $R_c/R_s=1$, and (c) $R_c/R_s=0.01$, where $d^*=d/R_s$. Here the solid line represents the energy calculated using (30), and the dot line denotes the energy calculated by Gu and Li [1999]. For reference, the energy between the sphere and a flat surface calculated by Hamaker [1937] is shown as the wide dot line.

calculated by Hamaker [1937], regardless of the distance between the sphere and the cylinder. That is, the curvature effect of the cylinder on the interaction energy is negligible and thus their assumption is valid. As R_c/R_s decreases, the curvature effect plays a very important role in the van der Waals interaction energy. However, Gu and Li's model does not capture the curvature effect of the cylinder at a relatively small distance d^* .

In a similar way, we calculate the interaction energy between a cylinder and a sphere inside the cylinder as shown in Fig. 5(b). We use the interaction energy of an atom inside a hollow cylinder $\phi_h(d, R)$ from (10). The total intersection can be expressed as (29) by replacing

$$t = R_c - d - R_s \tag{31}$$

In the case of $t \geq R_s$, we have the interaction as

$$\begin{aligned} \Phi_{ic}(d) &= \int_{r-R_s}^{r+R_s} \phi_h(R_c-r, R_c) \rho_s S dr = \int_{r-R_s}^{r+R_s} \\ &= \int_{r-R_s}^{r+R_s} \frac{4Ar\sqrt{(r+t)^2 - R_s^2}}{3\pi(r-R_c)^3(r+R_c)^3} \left\{ E\left[\frac{(r-t)^2 - R_s^2}{(r+t)^2 - R_s^2}\right] \right. \\ &\quad \left. - K\left[\frac{(r-t)^2 - R_s^2}{(r+t)^2 - R_s^2}\right] \right\} \times \left[\sqrt{rR_c(r^2 + 7R_c^2)} \operatorname{Re}\left[E\left[\frac{(r+R_c)^2}{4rR_c}\right]\right] \right. \\ &\quad \left. + R_c(r-3R_c)(r-R_c)K\left[-\frac{4rR_c}{(r-R_c)^2}\right] \right] dr \end{aligned} \quad (32)$$

When $t < R_s$, in r range of $0: (R_s-t)$, we will have a negative value of the intersection calculated by (29) and (31). Therefore, the interaction energy becomes

$$\begin{aligned} \Phi_{ic}(d) &= \int_0^{r+R_s} \phi_h(R_c-r, R_c) \rho_s |S| dr \\ &= \int_0^{R_s-t} \phi_h(R_c-r, R_c) \rho_s (-S) dr + \int_{R_s-t}^{r+R_s} \phi_h(R_c-r, R_c) \rho_s S dr \end{aligned} \quad (33)$$

DISCUSSION ON THE VAN DER WAALS INTERACTION ENERGIES IN CARBON NANOTUBES

In this section, we discuss interaction energies which might exist in two-dimensional carbon nanotubes and C_{60} molecules. They are two-dimensional in the sense that the carbon atoms reside only in an interface between two phases. Thus, the surface integral of (2) should be used to calculate the van der Waals interactions in CNTs. First, we calculate the van der Waals energies between a carbon

atom and a two-dimensional carbon nanotube, and between a carbon atom and a two-dimensional C_{60} molecule. Based on these, we calculate the interaction energies for several cases of CNT geometries.

1. van der Waals Interaction between a Carbon Atom and a SWCNT/ C_{60}

In Fig. 7, we illustrate three cases: a carbon atom outside a SWCNT, a carbon atom inside a SWCNT, and a carbon atom outside a C_{60} molecule. In order to calculate the interactions, we integrate (2) over the surface S :

$$\phi(d) = \iint_S -\frac{C}{r^6} \rho^{(\sigma)} ds \quad (34)$$

where $\rho^{(\sigma)}$ is the surface mass density, the number of carbon atoms in the unit surface area.

In the case of Fig. 7(a), we have

$$\begin{aligned} \phi_i(d, R_i) &= \int_0^{2\pi} \int_{-\infty}^{\infty} -\frac{C}{[(d+R_i)^2 + R_i^2 - 2(d+R_i)R_i \cos \theta + z^2]^3} \rho^{(\sigma)} R_i dz d\theta \\ &= -\frac{C\pi\rho^{(\sigma)}R_i}{2d^3(d+2R_i)^4} \left\{ 4(d^2 + 2dR_i + 2R_i^2)E\left[\frac{-4R_i(d+R_i)}{d^2}\right] \right. \\ &\quad \left. - (d+2R_i)^2 K\left[\frac{-4R_i(d+R_i)}{d^2}\right] \right\} \end{aligned} \quad (35)$$

and in the case of Fig. 7(b), we have

$$\begin{aligned} \phi_i(d, R_i) &= \int_0^{2\pi} \int_{-\infty}^{\infty} -\frac{C}{[(R_i-d)^2 + R_i^2 - 2(R_i-d)R_i \cos \theta + z^2]^3} \rho^{(\sigma)} R_i dz d\theta \\ &= -\frac{C\pi\rho^{(\sigma)}R_i}{2d^3(d-2R_i)^4} \left\{ 4(d^2 - 2dR_i + 2R_i^2)E\left[\frac{4R_i(d-R_i)}{d^2}\right] \right. \\ &\quad \left. - (d-2R_i)^2 K\left[\frac{4R_i(d-R_i)}{d^2}\right] \right\} \end{aligned} \quad (36)$$

The interaction energy between a carbon atom and a C_{60} molecule shown in Fig. 7(c) can be written as

$$\phi(d, R_f) = \iint_S -\frac{C}{[x^2 + y^2 + (z - R_f - d)^2]^3} \rho^{(\sigma)} ds \quad (37)$$

where

$$x^2 + y^2 + z^2 = R_f^2 \quad (38)$$

For a smooth function $H[x, y, z=f(x, y)]$ defined on S , the double integral of H over S can be expressed as a double integral in the xy -plane [Kaplan, 1991]:

$$\iint_S H ds = \iint_{\Sigma} H[x, y, f(x, y)] \sqrt{1 + \left(\frac{\partial z}{\partial x}\right)^2 + \left(\frac{\partial z}{\partial y}\right)^2} dx dy \quad (39)$$

where Σ is the projection of S on the xy -plane. Using (38), (39), and the change of variable [Kaplan, 1991], Eq. (37) becomes

$$\begin{aligned} \phi(d, R_f) &= \iint_{\Sigma} -\frac{C}{[x^2 + y^2 + (f(x, y) - R_f - d)^2]^3} \rho^{(\sigma)} \sqrt{1 + \left(\frac{\partial z}{\partial x}\right)^2 + \left(\frac{\partial z}{\partial y}\right)^2} dx dy \\ &= \int_0^{2\pi} \int_0^{R_f} -\frac{C}{[r^2 + (\sqrt{R_f^2 - r^2} - R_f - d)^2]^3} \frac{R_f}{\sqrt{R_f^2 - r^2}} \rho^{(\sigma)} r dr d\theta \end{aligned}$$

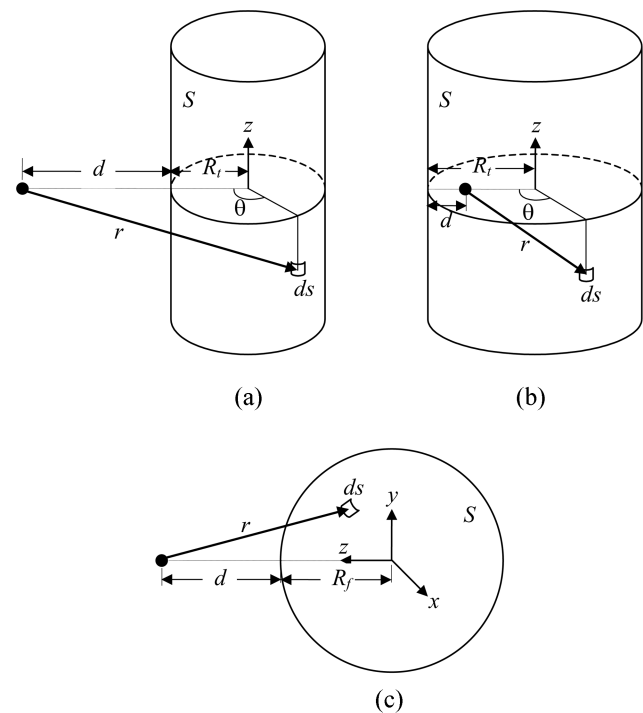


Fig. 7. van der Waals interactions of (a) a carbon atom outside a SWCNT, (b) a carbon atom inside a SWCNT, and (c) a carbon atom outside a C_{60} molecule. The distances r for (a), (b), and (c) are $\sqrt{(d+R_i)^2 + R_i^2 - 2(d+R_i)R_i \cos \theta + z^2}$, $\sqrt{(R_i-d)^2 + R_i^2 - 2(R_i-d)R_i \cos \theta + z^2}$, and $\sqrt{x^2 + y^2 + (z - R_f - d)^2}$.

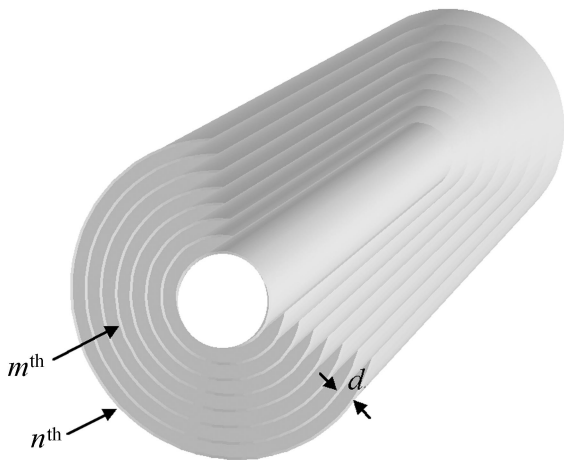


Fig. 8. Schematic of an n layer multi-walled carbon nanotube.

$$+ \int_0^{2\pi} \int_0^{R_i} \frac{C}{[r^2 + (-\sqrt{R_j^2 - r^2} - R_j - d)]^3 \sqrt{R_j^2 - r^2}} \rho^{(\sigma)} r dr d\theta$$

$$= -\frac{4C\pi\rho^{(\sigma)}R_j^2(d^2 + 2dR_j + 2R_j^2)}{d^4(d + 2R_j)^4} \quad (40)$$

2. van der Waals Interaction in a MWCNT

Now let us calculate the van der Waals interaction energy in an n -layer multi-walled carbon nanotube (MWCNT) shown in Fig. 8.

With the inner radius of R_i and the interlayer distance of d , the m^{th} layer is at a distance of $R_i + (m-1)d$ from the center. The surface cylinder of m^{th} the layer interacts with the other surface cylinders. When $i < m$, the interaction energy between the m^{th} layer and the i^{th} layer Φ_{mi} can be obtained using (35), while (36) is used when $i > m$. Thus, the interaction energy per unit surface area of the m^{th} layer becomes

$$\Phi_m = \sum_{i=1(i \neq m)}^n \Phi_{mi}$$

$$= \rho^{(\sigma)} \left\{ \sum_{i=1}^{m-1} \phi_i [(m-i)d, R_i + (i-1)d] + \sum_{i=m+1}^n \phi_i [(i-m)d, R_i + (i-1)d] \right\} \quad (41)$$

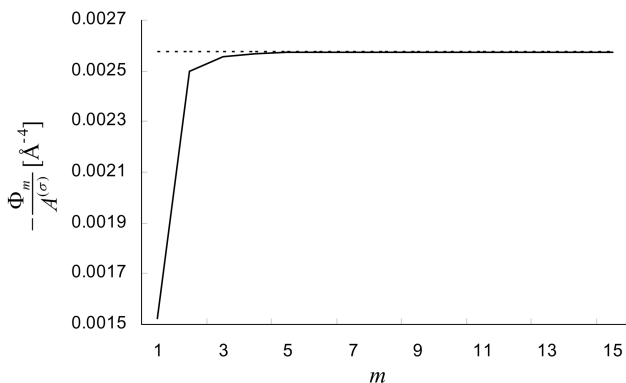


Fig. 9. van der Waals interaction energy in a 20-layer multi-walled carbon nanotubes with respect to layers. Here we have used $A^{(\sigma)} \equiv C\pi^2\rho^{(\sigma)}$. The dotted line indicates the van der Waals energy in graphite.

In Fig. 9, we illustrate the van der Waals interaction energy for a 20-layer MWCNT whose inner radius R_i is 1.0 nm. We have also taken $d=0.34$ nm, which is the interlayer distance of graphite. At low layers, the interaction energy stiffly increases as the layer increases. There is little change in the interaction energy at relatively high layers and the energy approaches the van der Waals energy of graphite.

3. van der Waals Interaction between Two SWCNTs Crossed at an Angle α

As shown in Fig. 1, CNTs are randomly oriented in a bundle of CNTs or in a polymer matrix. In understanding CNT mechanics, it is important to exactly estimate the interaction between two crossed CNTs. We again use Fig. 4(b). Since all of the carbon atoms reside in the surface, the distance between the differential surface element and the surface of the other SWCNT is given as, by using (22)

$$\overline{AC'} = \sqrt{(R_2 - R_2 \cos\theta + d + R_1)^2 + (z \sin\alpha - R_2 \sin\theta \cos\alpha)^2} - R_1 \quad (42)$$

From (35) and (42), we can express the interaction between two SWCNTs crossed at an angle α as

$$\Phi_{ii}(d) = \int_{-l}^l \int_0^{2\pi} \phi_i(\overline{AC'}, R_1) \rho^{(\sigma)} R_2 d\theta dz$$

$$= \int_{-l}^l \int_0^{2\pi} \frac{A^{(\sigma)} R_1 R_2}{2\pi(\overline{AC'})^3 (\overline{AC'} + 2R_1)^4} \left\{ 4[(\overline{AC'})^2 + 2(\overline{AC'})R_1 + 2R_1^2] E \left[-\frac{4R_1(\overline{AC'} + R_1)}{(\overline{AC'})^2} \right] - (\overline{AC'} + 2R_1)^2 K \left[-\frac{4R_1(\overline{AC'} + R_1)}{(\overline{AC'})^2} \right] \right\} d\theta dz \quad (43)$$

where

$$A^{(\sigma)} \equiv C\pi^2\rho^{(\sigma)} \quad (44)$$

4. van der Waals Interaction between C_{60} Molecules and Carbon Nanotubes

Very recently, C_{60} molecules encapsulated in carbon nanotubes, so-called peapods, have been discovered by Smith et al. [1998] and studied due to their unique electronic properties [Vavro et al., 2002; Hornbaker et al., 2002]. In the peapods, the van der Waals interaction may be a key factor to determine their structures, sizes, and properties [Okada et al., 2001; Hodak and Girifalco, 2001; Ulbricht et al., 2003]. The existing interactions in the peapods are illustrated in Fig. 10: C_{60} - C_{60} and C_{60} -SWCNT.

From a molecular point of view, the van der Waals interactions in the peapods have been studied by Lu et al. [1992] and Ulbricht et al. [2003]. Girifalco and Hodak [Girifalco, 1991, 1992; Girifalco et al., 2000; Hodak and Girifalco, 2002] have also obtained expressions for the interactions by using the double surface integral of the Lennard-Jones potential. In calculating the interaction, they used the smeared-out sphere approximation.

In this section, we calculate the van der Waals interactions in the peapods system without the assumption. For the C_{60} - C_{60} system depicted in Fig. 10(a), the distance between the surface element ds in the right- C_{60} and the surface of the left- C_{60} is $\sqrt{x^2 + y^2 + (z-t)^2} - R_p$, where $t=d+2R_p$. Using (40), we can write the net interaction between two C_{60} molecules as

$$\Phi_{ij}(d) = \iint_s \phi_j(\sqrt{x^2 + y^2 + (z-t)^2} - R_p, R_p) \rho^{(\sigma)} ds$$

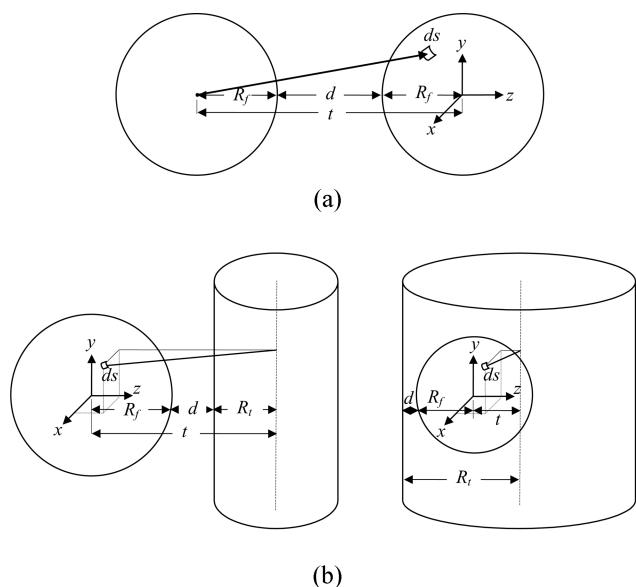


Fig. 10. van der Waals interactions in peapods: (a) the interaction between two C₆₀ molecules, (b) the interaction between a C₆₀ molecule and a SWCNT, and (c) the interaction between an encapsulated C₆₀ molecule and a SWCNT.

$$= \iint_S \frac{-4C\pi\rho^{(\sigma)2}R_f^2[x^2+y^2+(z-t)^2+R_f^2]}{[x^2+y^2+(z-t)^2-R_f^2]^4} ds \quad (45)$$

In view of (39) and the change of variables, this becomes

$$\begin{aligned} \Phi_{ff}(d) &= \iint_S \frac{-4C\pi\rho^{(\sigma)2}R_f^2[x^2+y^2+(z-t)^2+R_f^2]}{[x^2+y^2+(z-t)^2-R_f^2]^4} \sqrt{\frac{R_f^2}{R_f^2-x^2-y^2}} dx dy \\ &= \int_0^{2\pi} \int_0^{R_f} \frac{-4C\pi\rho^{(\sigma)2}R_f^2[r^2+(\sqrt{R_f^2-r^2}-t)^2+R_f^2]}{[r^2+(\sqrt{R_f^2-r^2}-t)^2+R_f^2]^4} \sqrt{\frac{R_f^2}{R_f^2-r^2}} r dr d\theta \\ &\quad + \int_0^{2\pi} \int_0^{R_f} \frac{-4C\pi\rho^{(\sigma)2}R_f^2[r^2+(-\sqrt{R_f^2-r^2}-t)^2+R_f^2]}{[r^2+(-\sqrt{R_f^2-r^2}-t)^2+R_f^2]^4} \sqrt{\frac{R_f^2}{R_f^2-r^2}} r dr d\theta \\ &= -\frac{16A^{(\sigma)}R_f^4(3d^4+24d^3R_f+66d^2R_f^2+72dR_f^3+32R_f^4)}{3d^3(d+2R_f)^4(d+4R_f)^3} \quad (46) \end{aligned}$$

This is identical to the result given in the paper of Girifalco [1992].

As seen in Fig. 10(b), the distance between the surface element ds in a C₆₀ molecule and the surface of a SWCNT is $\sqrt{x^2+(z-t)^2}-R_f$, where $t=d+R_f+R_f$. Thus, the interaction energy between the C₆₀ molecule and the SWCNT can be written as, by using (35) and (39)

$$\begin{aligned} \Phi_{ft}(d) &= \iint_S \phi_t(\sqrt{x^2+(z-t)^2}-R_f, R_f)\rho^{(\sigma)} ds \\ &= \int_0^{2\pi} \int_0^{R_f} \phi_t(\sqrt{r^2\cos^2\theta+(\sqrt{R_f^2-r^2}-t)^2}-R_f, R_f)\rho^{(\sigma)} \sqrt{\frac{R_f^2}{R_f^2-r^2}} r dr d\theta \\ &\quad + \int_0^{2\pi} \int_0^{R_f} \phi_t(\sqrt{r^2\cos^2\theta+(-\sqrt{R_f^2-r^2}-t)^2}-R_f, R_f)\rho^{(\sigma)} \sqrt{\frac{R_f^2}{R_f^2-r^2}} r dr d\theta \quad (47) \end{aligned}$$

For a C₆₀ molecule encapsulated in a SWCNT as shown in Fig. 10(c), the interaction can be expressed as

$$\begin{aligned} \Phi_{et}(d) &= \iint_S \phi_t(R_f-\sqrt{x^2+(z-t)^2}, R_f)\rho^{(\sigma)} ds \\ &= \int_0^{2\pi} \int_0^{R_f} \phi_t(R_f-\sqrt{r^2\cos^2\theta+(\sqrt{R_f^2-r^2}-t)^2}, R_f)\rho^{(\sigma)} \sqrt{\frac{R_f^2}{R_f^2-r^2}} r dr d\theta \\ &\quad + \int_0^{2\pi} \int_0^{R_f} \phi_t(R_f-\sqrt{r^2\cos^2\theta+(-\sqrt{R_f^2-r^2}-t)^2}, R_f)\rho^{(\sigma)} \sqrt{\frac{R_f^2}{R_f^2-r^2}} r dr d\theta \quad (48) \end{aligned}$$

where ϕ is in (36) and $t=R_f-(d+R_f)$.

For these cases, the van der Waals energies calculated from data given by Girifalco et al. [2000] are listed in Table 1. For some of the systems, the interaction energies are equal to those calculated numerically by using Eqs. (7) and (10) in the paper of Girifalco et al. [2000].

Note that for each system the surface Hamaker constant defined in (44) is slightly different from the graphene-graphene system [Girifalco et al., 2000; Hodak and Girifalco, 2001].

CONCLUSIONS

For the van der Waals interaction energies of several non-planar bodies, we have obtained simple analytic expressions without assum-

Table 1. van der Waals interaction energies in a peapods system

System	Radius (R_f, R_t) ^a Å	Equil. spacing (d) ^a Å	Energy ($\Phi/A^{(\sigma)}$) ^a Å ⁻²	Energy ($\Phi/A^{(\sigma)}$) ^a Å ⁻²	
C ₆₀ -C ₆₀	3.55	2.95	-0.0155 ^b	-0.0155 ^f	
C ₆₀ -(10, 10) tube	3.55, 6.785	2.945	-0.0329 ^c	-0.0329 ^g	
Encap. C ₆₀ -(10, 10) tube	3.55, 6.785	3.235	-0.2030 ^d	-	
(10, 10)-(10, 10) tube	6.785	3.154	$\alpha=0$	-0.0069 ^e	-0.0069 ^g
			$\alpha=45^\circ$	-0.0076 ^e	-
			$\alpha=90^\circ$	-0.0086 ^e	-

^aGiven by Girifalco et al. [2000].

^bCalculated using (46).

^cCalculated using (47).

^dCalculated using (48).

^eCalculated using (43).

^fCalculated using an expression given by Girifalco [1992].

^gCalculated using expressions given by Girifalco et al. [2000].

ing that the distance between non-planar bodies is much smaller than the radii of the non-planar bodies. Thus, one can easily compute the interaction energies between non-planar bodies without a complicated numerical integration tool. Also, the results could be applied to nanoscale non-planar materials like nanowires.

From the continuum approach, we have also obtained the van der Waals interaction energies between carbon atoms and two-dimensional carbon nanotubes including C_{60} molecules. Based on these, we calculated the interaction energy for multi-walled carbon nanotubes. In the MWCNT, the interaction energy quickly approaches that of graphite as the number of layers increases. We also obtained the interaction energy between two SWCNTs crossed by an angle. For the peapods system, where C_{60} molecules are encapsulated in carbon nanotubes, we have computed the van der Waals interaction energies using the magnitude for an equilibrium spacing given by Girifalco et al. [2000].

NOMENCLATURE

- A : Hamaker constant defined by (13)
 $A^{(\sigma)}$: surface Hamaker constant defined by (44)
 C : London dispersion force coefficient
 d : distance between an atom and a body or between two bodies
 ds : differential surface element
 ${}_pF_q$: generalized hypergeometric series defined as (17)
 $G_{p,q}^{m,m}$: Meijer's G function defined as (19)
 R : radius
 S : intersection between a cylinder of radius r and a sphere of radius R_s or surface of carbon nanotubes
 t : center-to-center distance

Greek Letters

- α : angle between two crossed cylinders
 ρ : constant number density of a body
 $\rho^{(\sigma)}$: constant number of carbon atoms in unit surface area
 ϕ : interaction energy between an atom and a non-planar body
 Φ : interaction energy between two non-planar bodies

REFERENCES

- Abramowitz, M. and Stegun, I. A., "Handbook of Mathematical Functions with Formulas, Graphs, and Mathematical Tables," National Bureau of Standards, Washington (1972).
 Adamczyk, Z. and van de Ven, T. G. M., "Deposition of Brownian Particles onto Cylindrical Collectors," *J. Colloid Interface Sci.*, **84**, 497 (1981).
 Bhattacharjee, S. and Sharma, A., "Interaction Energy of Particles in Porous Media: New Deryaguin Type Approximation," *Langmuir*, **12**, 5498 (1996).
 Bhattacharjee, S. and Sharma, A., "Apolar, Polar, and Electrostatic Interactions of Spherical Particles in Cylindrical Pores," *J. Colloid Interface Sci.*, **187**, 83 (1997).
 Boustimi, M., Baudon, J., Candori, P. and Robert, J., "van der Waals Interaction between an Atom and a Metallic Nanowire," *Phys. Rev. B*, **65**, 155402 (2002).
 Chang, Y. I. and Wang, Y. F., "Adhesion of an Elastic Particle to a Plane

- Surface: Effects of the Inertial Force and the van der Waals Force," *Colloids and surfaces A*, **111**, 21 (1996).
 Dzyaloshinskii, I. E., Lifshitz, E. M. and Pitaevskii, L. P., "The General Theory of van der Waals Forces," *Adv. Phys.*, **10**, 165 (1961).
 Girifalco, L. A., "Interaction Potential for C_{60} Molecules," *J. Phys. Chem.*, **95**, 5370 (1991).
 Girifalco, L. A., "Molecular Properties of C_{60} in the Gas and Solid Phases," *J. Phys. Chem.*, **96**, 858 (1992).
 Girifalco, L. A., Hodak, M. and Lee, R. S., "Carbon Nanotube, Buckyballs, Ropes, and a Universal Graphitic Potential," *Phys. Rev. B*, **62**, 13104 (2000).
 Gradshteyn, I. S. and Ryzhik, I. M., "Table of Integrals, Series, and Products," Academic Press, New York (1965).
 Gu, Y. and Li, D., "The van der Waals Interaction between a Spherical Particle and a Cylinder," *J. Colloid Interface Sci.*, **217**, 60 (1999).
 Gu, Y. and Li, D., "Deposition of Spherical Particles onto Cylindrical Solid Surfaces," *J. Colloid Interface Sci.*, **248**, 315 (2002).
 Hamaker, H. C., "The London-van der Waals Attraction between Spherical Particles," *Physica*, **4**, 1058 (1937).
 Henrard, L., Hernandez, E., Bernier, P. and Rubio, A., "van der Waals Interaction in Nanotube Bundles: Consequences on Vibrational Modes," *Phys. Rev. B*, **60**, R8521 (1999).
 Hirschfelder, J. O., Curtiss, C. F. and Bird, R. B., "Molecular Theory of Gases and Liquids," Wiley, New York (1954).
 Hodak, M. and Girifalco, L. A., "Fullerenes Inside Carbon Nanotubes and Multi-walled Carbon Nanotubes: Optimum and Maximum Sizes," *Chem. Phys. Lett.*, **350**, 405 (2001).
 Hodak, M. and Girifalco, L. A., "Cohesive Properties of Fullerene-filled Nanotube Ropes," *Chem. Phys. Lett.*, **363**, 93 (2002).
 Hornbaker, D. J., Kahng, S. J., Misra, S., Smith, B. W., Johnson, A. T., Mele, E. J., Luzzi, D. E. and Yazdani, A., "Mapping the One-dimensional Electronic States of Nanotube Peapod Structures," *Science*, **295**, 828 (2002).
 Hough, D. B. and White, L. R., "The Calculation of Hamaker Constants from Lifshitz Theory with Applications to Wetting Phenomena," *Adv. Colloid Interface Sci.*, **14**, 3 (1980).
 Hummer, G., Rasaiah, J. C. and Noworyta, J. P., "Water Conduction through the Hydrophobic Channel of a Carbon Nanotube," *Nature*, **414**, 188 (2001).
 Iijima, S., "Helical Microtubules of Graphitic Carbon," *Nature*, **354**, 56 (1991).
 Israelachvili, J. N., "van der Waals Dispersion Force Contribution to Works of Adhesion and Contact Angles on Basis of Macroscopic Theory," *J. Chem. Soc. Faraday Trans. II*, **69**, 1729 (1973).
 Israelachvili, J. N., "Intermolecular and Surface Forces," Academic Press, London (1991).
 Kaplan, W., "Advanced Calculus," Addison-Wesley Publishing Company, Massachusetts (1991).
 Lifshitz, E. M., "The Theory of Molecular Attractive Forces Between Solids," *Soviet Phys. JETP (Engl. Transl.)*, **2**, 73 (1956).
 Lu, J. P., Li, X. P. and Martin, R. M., "Ground State and Phase Transitions in Solid C_{60} ," *Phys. Rev. Lett.*, **68**, 1551 (1992).
 Mahanty, J. and Ninham, B. W., "Dispersion Forces," Academic Press, New York (1976).
 Mendeleev, M. I., Srolovitz, D. J., Safran, S. A. and Tenne, R., "Equilibrium Structure of Multilayer van der Waals Films and Nanotubes," *Phys. Rev. B*, **65**, 075402 (2002).

- Odom, T. W., Huang, J. L., Kim, P. and Lieber, C. M., "Atomic-structure and Electronic Properties of Single-walled Carbon Nanotubes," *Nature*, **391**, 62 (1998).
- Okada, S., Saito, S. and Oshiyama, A., "Energetics and Electronic Structures of Encapsulated C_{60} in a Carbon Nanotube," *Phys. Rev. Lett.*, **86**, 3835 (2001).
- Qian, D., Liu, W. K. and Ruoff, R. S., "Mechanics of C_{60} in Nanotubes," *J. Phys. Chem. B*, **105**, 10753 (2001).
- Qin, L.-C. and Iijima, S., "Structure and Formation of Raft-like Bundles of Single-walled Helical Carbon Nanotubes Produced by Laser Evaporation," *Chem. Phys. Lett.*, **269**, 65 (1997).
- Smith, B. W., Monthieux, M. and Luzzi, D. E., "Encapsulated C_{60} in Carbon Nanotube," *Nature*, **396**, 323 (1998).
- Ulbricht, H., Moos, G. M. and Hertel, T., "Interaction of C_{60} with Carbon Nanotubes and Graphite," *Phys. Rev. Lett.*, **90**, 095501 (2003).
- Vavro, J., Llaguno, M. C., Satishkumar, B. C., Luzzi, D. E. and Fischer, J. E., "Electrical and Thermal Properties of C_{60} -filled Single-wall Carbon Nanotubes," *Appl. Phys. Lett.*, **80**, 1450 (2002).
- Wildoer, J. W. G., Venema, L. C., Rinzler, A. G., Smalley, R. E. and Dekker, C., "Electronic Structure of Atomically Resolved Carbon Nanotube," *Nature*, **391**, 59 (1998).
- Yakobson, B. I., Brabec, C. J. and Bernholc, J., "Nanomechanics of Carbon Tubes: Instabilities Beyond Linear Response," *Phys. Rev. Lett.*, **76**, 2511 (1996).
- Yu, M. F., Lourie, O., Dyer, M. J., Moloni, K., Kelly, T. F. and Ruoff, R. S., "Strength and Breaking Mechanism of Multiwalled Carbon Nanotubes Under Tensile Load," *Science*, **287**, 637 (2000).